British Journal of Pharmacology (2005) 144, 252–264
www.nature.com/bjp

Role of basal extracellular Ca^{2+} entry during 5-HT-induced vasoconstriction of canine pulmonary arteries

[1,2]Sean M. Wilson, [1,3]Helen S. Mason, [1]Lih C. Ng, [1]Stephen Montague, [1]Louise Johnston, [1]Neil Nicholson, [1]Sarah Mansfield & *,[1]Joseph R. Hume

[1]Department of Pharmacology, University of Nevada School of Medicine, Reno, MS 318, NV 89557, U.S.A.

1 Measurements of artery contraction, cytosolic [Ca^{2+}], and Ca^{2+} permeability were made to examine contractile and cytosolic [Ca^{2+}] responses of canine pulmonary arteries and isolated cells to 5-hydroxytryptamine (5-HT), and to determine the roles of intracellular Ca^{2+} release and extracellular Ca^{2+} entry in 5-HT responses.

2 The EC_{50} for 5-HT-mediated contractions and cytosolic [Ca^{2+}] increases was $\sim 10^{-7}$ M and responses were inhibited by ketanserin, a 5-HT_{2A}-receptor antagonist.

3 5-HT induced cytosolic [Ca^{2+}] increases were blocked by 20 μM Xestospongin-C and by 2-APB ($IC_{50} = 32\,\mu$M), inhibitors of $InsP_3$ receptor activation.

4 5-HT-mediated contractions were reliant on release of $InsP_3$ but not ryanodine-sensitive Ca^{2+} stores.

5 5-HT-mediated contractions and cytosolic [Ca^{2+}] increases were partially inhibited by 10 μM nisoldipine, a voltage-dependent Ca^{2+} channel blocker.

6 Extracellular Ca^{2+} removal reduced 5-HT-mediated contractions further than nisoldipine and ablated cytosolic [Ca^{2+}] increases and [Ca^{2+}] oscillations. Similar to Ca^{2+} removal, Ni^{2+} reduced cytosolic [Ca^{2+}] and [Ca^{2+}] oscillations.

7 Mn^{2+} quench of fura-2 and voltage-clamp experiments showed that 5-HT failed to activate any significant voltage-independent Ca^{2+} entry pathways, including store-operated and receptor-activated nonselective cation channels. Ni^{2+} but not nisoldipine or Gd^{3+} blocked basal Mn^{2+} entry.

8 Voltage-clamp experiments showed that simultaneous depletion of both $InsP_3$ and ryanodine-sensitive intracellular Ca^{2+} stores activates a current with linear voltage dependence and a reversal potential consistent with it being a nonselective cation channel. 5-HT did not activate this current.

9 Basal Ca^{2+} entry, rather than CCE, is important to maintain 5-HT-induced cytosolic [Ca^{2+}] responses and contraction in canine pulmonary artery.
British Journal of Pharmacology (2005) **144,** 252–264. doi:10.1038/sj.bjp.0706077
Published online 10 January 2005

Keywords: Smooth muscle; serotonin; sarcoplasmic reticulum; fura-2; intracellular [Ca^{2+}]

Abbreviations: 4-AP, 4-aminopyridine; BAPTA, 1,2-bis(2-aminophenoxy)-ethane-*N*,*N*,*N*′,*N*′-tetra acetic acid; CCE, capacitative calcium entry; CICR, calcium-induced calcium release; CPA, cyclopiazonic acid; I_{NSC}, neural–humoral activated cation channels; $InsP_3$, inositol 1,4,5-tri-phosphate; K-H, Krebs–Henseleit solutionNCCE, noncapacitative calcium entry; PASMC, pulmonary arterial smooth muscle cell; PE, phenylephrine; PSS, physiological saline solution; SERCA, sarcoplasmic-endoplasmic reticulum Ca^{2+} ATPase; SR, sarcoplasmic reticulum, store-depletion-activated cation channels (I_{SOC}); T_{kmax}, contraction of pulmonary artery rings in response to 50–60 mM K^+

Introduction

5-Hydroxytryptamine (5-HT) is a potent mediator of pulmonary hypertension by stimulating increases in pulmonary arterial smooth muscle cell (PASMC) contraction and proliferation (McGoon & Vanhoutte, 1984; MacLean *et al*., 2000). 5-HT-induced contractions are predominately mediated by increased intracellular [Ca^{2+}] (Yuan *et al*., 1997) through activation of membrane-bound G-protein coupled receptors that are associated with phospholipase C. The resulting phosphoinositide hydrolysis produces inositol 1,4,5-triphosphate ($InsP_3$) (Yang *et al*., 1997) and diacylglycerol (DAG). These second messengers and the systems they are linked to often activate xestospongin-C (XeC) (Gafni *et al*., 1997; Kiselyov *et al*., 1998) and 2-APB (Ma *et al*., 2000; Wu *et al*., 2000) inhibitable sarcoplasmic reticulum (SR) $InsP_3$-sensitive Ca^{2+} channels, as well as sarcolemmal voltage-dependent and voltage-independent Ca^{2+}-permeable channels (Kuriyama *et al*., 1998).

Smooth muscle cells typically have both ryanodine and $InsP_3$ receptors on their SR and canine PASMCs are no exception (Jabr *et al*., 1997; Janiak *et al*., 2001). The corresponding $InsP_3$- and ryanodine-sensitive SR Ca^{2+} stores often exhibit some functional overlap; however, we have found through a series of contractile and imaging studies that the

*Author for correspondence; E-mail: joeh@med.unr.edu
[2]Current address: Department of Pharmacology, School of Pharmacy, University of Mississippi, University, P.O. Box 1848, MS 38677, U.S.A.
[3]Current address: Cardiff School of Biosciences, Cardiff University, Biomedical Sciences Bldg, Museum Avenue, Cardiff, CF10 3US U.K.
Published online 10 January 2005

ryanodine- and $InsP_3$-sensitive SR Ca^{2+} stores are functionally independent in canine PASMCs (Jabr *et al*., 1997; Janiak *et al*., 2001).

Na^+- and Ca^{2+}-permeable nonselective cation channels may have important roles to smooth muscle contractility. Activation of these channels may facilitate smooth muscle contractility by providing a Ca^{2+} influx pathway and by causing membrane depolarization leading to activation of L-type, voltage-dependent, Ca^{2+} channels. Although the mechanisms for activation of nonselective cation channels remain unclear, they can be categorized into three separate classes: those that are constitutively active (Albert *et al*., 2003), those activated by neural–hormonal stimulation (Large, 1991) (I_{NSC}), or those activated following depletion of the intracellular Ca^{2+} stores (Ng & Gurney, 2001) (I_{SOC}).

Intracellular [Ca^{2+}] increases induced by 5-HT in rat PASMCs consist of an early transient phase, attributed to intracellular Ca^{2+} stores release, and a secondary, sustained phase, due to enhanced sarcolemmal Ca^{2+} influx (Yuan *et al*., 1997). A similar biphasic change in intracellular [Ca^{2+}] has been observed in PASMCs exposed to phenylephrine (PE), with the secondary sustained phase of elevated intracellular [Ca^{2+}] linked to activation of a Ca^{2+} store-depletion induced-sarcolemmal Ca^{2+} entry pathway (McDaniel *et al*., 2001). In canine PASMCs, we have recently shown that CCE is activated only when the functionally independent $InsP_3$- and ryanodine-sensitive Ca^{2+} stores are simultaneously depleted (Wilson *et al*., 2002b). However, the type or types of extracellular Ca^{2+} entry pathways activated by 5-HT in canine PASMCs have not been characterized. The purposes of the present experiments are: (1) to characterize the 5-HT contractile responses of small branches of canine pulmonary arteries, (2) to examine the role of 5-HT-induced Ca^{2+} release from intracellular stores, and (3) to identify which extracellular Ca^+ entry pathways are activated by 5-HT in canine PASMCs. Preliminary reports of these results have been presented (Wilson *et al*., 2002a).

Methods

Artery and cell isolation

Canine pulmonary arterial rings and individual smooth muscle cells were isolated as described previously (Jabr *et al*., 1997; Janiak *et al*., 2001). Mongrel dogs of either sex were euthanized with pentobarbital sodium (45 mg kg^{-1} i.v.) and ketamine (15 mg kg^{-1} i.v.), as approved by the University of Nevada at the Reno Institutional Animal Care and Use Committee. The heart and lungs were excised en block. Prior to isolation the main pulmonary arteries were flushed with a low-[Ca^{2+}] physiological saline solution (PSS) containing in mM: 125 NaCl; 5.36 KCl; 0.336 Na_2HPO_4; 0.44 K_2HPO_4; 11 HEPES; 1.2 $MgCl_2$; 0.05 $CaCl_2$; 10 glucose; 2.9 sucrose, pH 7.4 (adjusted with Tris); osmolarity 300 mOsm (adjusted with sucrose). The PSS was continuously bubbled with 100% O_2 during dissections to provide free O_2 at low temperatures. The third and fourth branches of pulmonary arteries were dissected at 5°C to decrease cellular metabolic activity. Vessels to be used for contractile studies were cleaned of all connective tissue and rings were cut and placed in cold Krebs-Henseleit (K-H) solution containing in mM: 120 NaCl; 4.8 KCl; 1.2 K_2HPO_4; 25 $NaHCO_3$; 1.2 $MgCl_2$; 2.5 $CaCl_2$; 5 glucose; osmolarity 300 mOsm (adjusted with sucrose). The K-H solution was continuously bubbled with 95% O_2 and 5% CO_2 to maintain pH at 7.4. Arteries to be used to isolate individual smooth muscle cells were cleaned of connective tissue, cut into small pieces, and placed in a tube containing fresh PSS. Tissue was immediately digested or stored in the refrigerator (5°C) for up to 24 h. To disperse cells, tissue was placed in low-[Ca^{2+}] PSS containing (in mg ml^{-1}): 0.5 collagenase type XI, 0.03 elastase type IV, and 0.5 bovine serum albumin for 14–16 h at 5°C. The tissue was then washed several times with 5°C low-[Ca^{2+}] PSS and tritrated with a fire-polished Pasteur pipette. The resulting dispersed canine PASMCs were then stored at 5°C for up to 8 h until experiments were performed.

Artery tension measurements

Artery tension measurements were performed as described previously (Jabr *et al*., 1997). Specifically, arterial rings were suspended in 10 ml organ chambers maintained at 37°C and bubbled with 95% O_2 and 5% CO_2 to maintain pH at 7.4. The ring segments were mounted on two triangular tungsten wires suspended between stainless steel wire hooks, one of which was anchored to the organ bath and the other connected to a force displacement transducer (Grass-Telefactor model FT03, West Warwick, RI, U.S.A.). Tension was continuously recorded and digitized on-line with a MP100WS data acquisition and analysis system (Biopac Systems, Inc., Goleta, CA, U.S.A.) connected to an IBM compatible computer.

Prior to the start of each experiment, arterial rings were allowed to equilibrate for 60 min during which time tissues were washed with fresh K-H solution at 10–15 min intervals. During the equilibration period, a resting tension of 0.75 g was placed on the rings. After this equilibration period, the viability of the tissue was tested by recording the response to a high K^+ K-H solution, where 50–60 mM KCl replaced equimolar NaCl. This concentration of KCl was previously determined to be the lowest capable of developing a maximal contraction (Jabr *et al*., 1997). Subsequently, all other contractions were expressed as a percentage of this maximal KCl contraction (T_{kmax}) in each individual arterial ring, thus allowing each tissue to be its own control. Most contractile studies were performed in arteries denuded of their endothelium, except for arteries used to construct a dose–response relationship for 5-HT (Figure 1) and those exposed to Gd^{3+} (Figure 3). Given that the presence of endothelium did not alter the EC_{50} for 5-HT-induced contractions relative to [Ca^{2+}], it seems unlikely that the presence of endothelium would affect the studies involving Gd^{3+}. The presence or absence of endothelium was determined by the relaxant response to acetylcholine (Ach; 10^{-7}, 10^{-6}, and 10^{-5} M) in rings precontracted with PE (10^{-6} M). Relaxation to Ach was observed only in arterial rings with a functional endothelium (Furchgott & Zawadzki, 1980).

Fluorescence imaging

Global [Ca^{2+}] measurements Cytosolic [Ca^{2+}] was measured in canine PASMCs loaded with the ratiometric Ca^{2+}-sensitive dye fura-2 AM (Molecular Probes, Eugene, OR, U.S. A.) using a dual excitation digital Ca^{2+}-imaging system (IonOptix

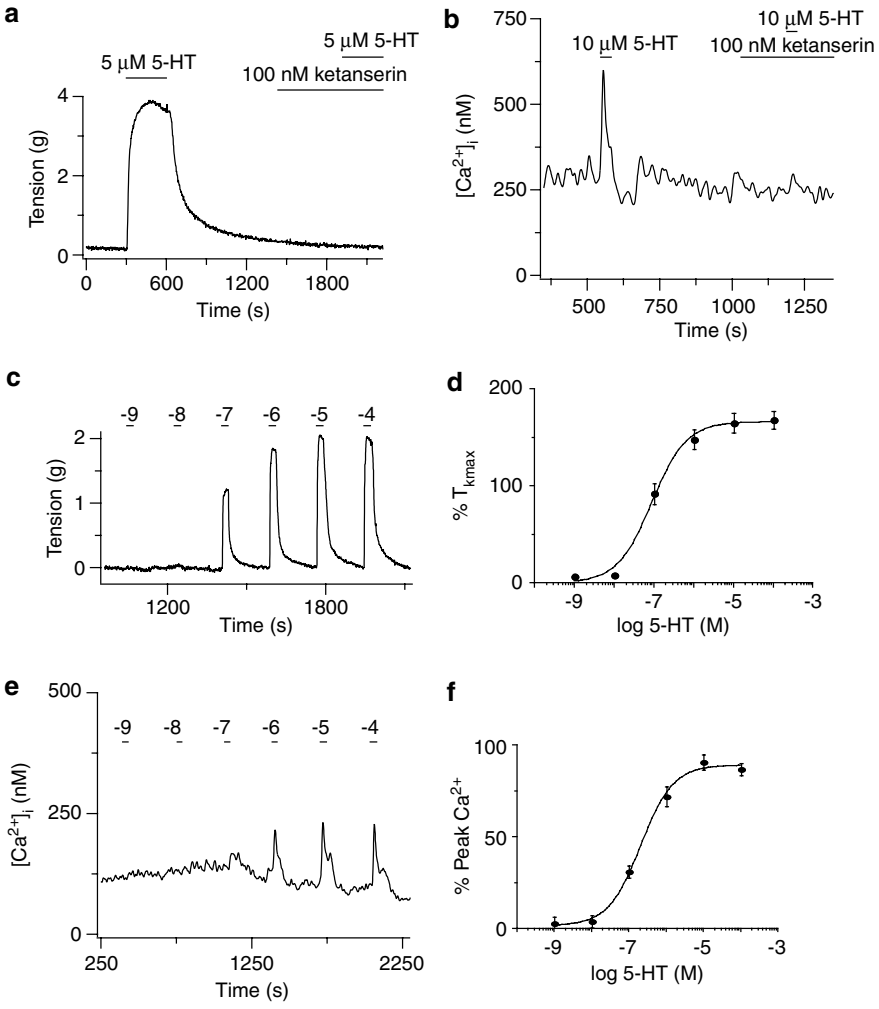

Figure 1 5-HT_{2A} receptor activation induces contraction of pulmonary artery rings and Ca^{2+} release in individual smooth muscle cells. (a) Isometric tension recording from an arterial ring exposed to 5 μM 5-HT in the absence and presence of 100 nM ketanserin. (b) Cytosolic [Ca^{2+}] recording from an individual pulmonary ASMC exposed to 10 μM 5-HT in the absence and presence of 0.1 μM ketanserin. (c) Isometric tension recording from an arterial ring exposed to 10^{-9} to 10^{-4} M 5-HT. (d) Dose–response relationship for 5-HT-induced contractions fit with a Hill equation (solid line) (equation (1)), $EC_{50} = 9 \times 10^{-8}$ M. Values are means of % T_{kmax} for nine arteries from three animals. (e) Cytosolic [Ca^{2+}] recording from an individual smooth muscle cell exposed to 10^{-9} to 10^{-4} M 5-HT. (f) Dose–response relationship for the peak of the 5-HT-induced Ca^{2+} release fit with an $EC_{50} = 2.1 \times 10^{-7}$ M (solid line) (equation (1)). Values are means of % peak [Ca^{2+}] for 15 cells from a single animal. Agonists were present during the times shown by the bars. Error bars represent $\pm$s.e.m.

Inc., Milton, MA, U.S.A.) equipped with an intensified CCD camera. The imaging system was mounted on an inverted microscope (Nikon) outfitted with a $\times 40$ (NA 1.3, Nikon Inc., Melville, NY, U.S.A.) oil immersion objective. Fura-2 AM was dissolved in DMSO and added from a 1 mM stock to the cell suspension at a final concentration of 10 μM. Cells were loaded with fura-2 AM for 15 min at 34°C and an additional 20 min in a perfusion chamber (Warner Instruments, Hamden, CT or Medical Systems Corp., Greenvale, NY, U.S.A.) at room temperature in the dark. In some experiments, cells were loaded with fura-2 AM for 20–30 min at room temperature in the dark. Results of experiments performed with either loading protocol were similar and thus were pooled. Cells were then washed for 30 min to allow for dye de-esterification at a flow rate of 1–2 ml min^{-1} with a balanced salt solution of the following composition (mM): 126 NaCl; 5 KCl; 0.3 NaH_2PO_4; 10 HEPES; 1 $MgCl_2$; 2 $CaCl_2$; 10 glucose; pH 7.4 (adjusted with NaOH) 285–305 mOsm. This range in osmolarities is under 10%, and is far less than the 20% decrease in osmolarity that has been shown to affect Ca^{2+} influx (Welsh *et al*., 2000). Cells were illuminated with a xenon arc lamp at wavelengths of 340 ± 15 and 380 ± 12 nm (Omega Optical, Brattleboro, VT, U.S.A.) and emitted light was collected from regions that encompassed single cells with a CCD camera at a wavelength of 510 nm (Nikon Inc., Melville, NY, U.S.A.). If cells contracted, the experiment was paused and the regions of interest resized. In most experiments, images were acquired at 1 Hz and stored on either compact disk or magnetic media for later analysis. Although it is difficult to precisely measure intracellular [Ca^{2+}] (Baylor & Hollingworth, 2000), *in situ* calibrations of fura-2 for each cell and [Ca^{2+}] estimates were made from the relation $[Ca^{2+}] = K_d \times (Sf_2/Sb_2) \times (R - R_{min})/(R_{max} - R)$, where R_{min} and R_{max} are the F_{340}/F_{380} ratios of Ca^{2+}-free and Ca^{2+}-saturated fura-2, respectively, Sf_2 is F_{380} of Ca^{2+}-free fura-2 and Sb_2 is F_{380} of Ca^{2+}-bound fura-2. The values for Sf_2 and R_{min} were determined by bathing cells in a balanced salt solution that did not have any added Ca^{2+} and

contained 10 mM EGTA and 1 μM ionomycin. The values for Sb_2 and R_{max} values were determined by perfusing cells with a balanced salt solution that contained 10 mM Ca^{2+} and 1 μM ionomycin. The K_d for fura-2 was assumed to be 224 nM (Grynkiewicz *et al*., 1985). During the [Ca^{2+}] calibration, 5 mM 2,3 butanedione monoxime was added to the bathing solution to inhibit smooth muscle contraction (Waurick *et al*., 1999). Experimental temperature was maintained at 29–32°C with a dual automatic temperature controller (Warner Instruments, Hamden, CT, U.S.A.).

Mn^{2+} quench The rate at which 100 μM Mn^{2+} quenched the fura-2 fluorescent signal was determined by regression analysis of fluorescent intensity (in arbitrary units) over time for cells excited at a wavelength of 357 ± 10 nm and emitted light collected at a wavelength of 510 nm (expressed as FI s^{-1}). After a 3–5 min control-recording period in the presence of 2 mM extracellular Ca^{2+}, cells were placed into a Ca^{2+}-free balanced salt solution that did not have any added Ca^{2+} or EGTA. Cells were analyzed only if the fluorescent intensity did not decrease in the absence of extracellular Ca^{2+} and if the rate of fura-2 quench by Mn^{2+} in the presence of 1 μM ionomycin was at least four-fold greater than the basal rate. Background fluorescence was collected automatically and subtracted from the acquired fluorescence video images during each experiment. Experimental temperature was 22–25°C.

Electrophysiology

A drop of canine PASMC suspension was placed in the bath chamber and left for several minutes to allow the cells to adhere to the bottom of the chamber. Currents were recorded from single cells at 22–25°C using dialyzed whole-cell patch clamp recording techniques (Hamill *et al*., 1981; Rae *et al*., 1991; Ahn & Hume, 1997). Pipettes with resistances of 3–6 Mohm were pulled from thin-walled borosilicate glass capillaries (Sutter Instruments Inc., Novato, CA, U.S.A.) and fire-polished. Cells were perfused by gravity feed at 1–2 ml min^{-1} with a balanced salt solution (as described above). To examine the effect of 5-HT on nonselective cation currents, pipettes were filled with a solution containing (in mM): 75 glutamic acid; 55 CsCl; 1 K_2HPO_4; 0.5 NaGTP; 5 MgATP; 10 EGTA; 10 HEPES; 5 glucose; pH 7.2 (adjusted with CsOH); 285–305 mOsm (adjusted with mannitol).

To examine the activation of store-depletion-induced currents in isolation, cells were perfused with a bath solution containing (in mM) 138 Na-methanesulfonate, 2 $Ca(OH)_2$, 10 HEPES, 10 glucose (pH was adjusted to 7.4 with NaOH and the osmolarity was adjusted to 285–300 mOsm with mannitol). In experiments where cells were exposed to Ni^{2+}, cells were perfused with a nominal Ca^{2+}-free solution in which the $Ca(OH)_2$ was replaced with equimolar Na-methanesulfonate. The pipette solution was (in mM): 140 Cs-aspartate, 3.2 $MgCl_2$, 12 1,2-bis(2-aminophenoxy)-ethane-*N*,*N*,*N*′,*N*′-tetra acetic acid (BAPTA), 10 HEPES (pH was adjusted to 7.2 with CsOH and the osmolarity was adjusted to 285–300 mOsm with mannitol). BAPTA (10 mM) was added to the pipette solution in order to minimize inactivation of the store-operated calcium currents (Zweifach & Lewis, 1995). Junction potentials associated with either pipette solution were <5 mV and were not compensated for.

The voltage offset between the patch pipette and the bath solution was nulled immediately before membrane rupture and the junction potential did not drift in the presence of low extracellular Cl^-. After gaining the whole-cell configuration, the series resistance was routinely compensated (~80%). Voltage steps were driven by pCLAMP 8.0 software (Axon Instruments, Union City, CA, U.S.A.). Cells were voltage-clamped at 0 mV to facilitate inactivation of voltage-dependent ion currents. Membrane currents were recorded using an Axopatch-1D amplifier (Axon Instruments), filtered at 2 kHz, connected to a microcomputer *via* an analogue-to-digital converter (Digidata 1322A, Axon Instruments). Data were analyzed using pCLAMP 8.0 (Axon Instruments) and Origin software (Microcal, Northampton, MA, U.S.A.). Experimental temperature was 22–25°C.

Chemicals and drugs

Ionomycin free acid was purchased from Calbiochem (San Diego, CA, U.S.A.) and nisoldipine was kindly provided by Miles Inc. (West Haven, CT, U.S.A.); all enzymes and other chemicals were purchased from Sigma (St Louis, MO, U.S.A.).

Analysis of data

Concentration–response curves for 5-HT (Figure 1) were fitted to a classical 'Hill equation': $E/E_{max} = [A]^n/([A]^n + EC_{50}[M]^n$, where E/E_{max} is the relative response to the agonist concentration, A[M]. EC_{50}[M] is the concentration of agonist required to give half-maximal response and n is the 'Hill coefficient'. Concentration–response curves with 2-APB as antagonist of 5-HT responses (Figure 2) were obtained by measuring the peak 5-HT-induced increase in [Ca^{2+}] ($\Delta[Ca^{2+}]$) at each antagonist concentration and the experimental data were fitted to the equation: $\Delta[Ca^{2+}]/\Delta[Ca^{2+}]_{max} = 1/[1 + ([A]/IC_{50}[M])^n]$, where $\Delta[Ca^{2+}]/\Delta[Ca^{2+}]_{max}$ represents the relative peak increase in $\Delta[Ca^{2+}]$, [A] is the antagonist concentration, IC_{50}[M] is the antagonist concentration giving half-maximal inhibition, and n is the 'Hill coefficient'.

All data are presented as mean ± s.e.m. Statistical difference within groups was determined with a two-tailed paired Student's *t*-test and between groups with a one-way analysis of variance (ANOVA) with a Student–Newman–Keuls (SNK) multiple comparison procedure. In cases where the data were not normally distributed, a Wilcoxon signed rank sum test was used to test for differences within groups and a Friedman repeated-measures ANOVA on ranks with a SNK multiple comparison procedure between groups. The specific test used for each data set is noted in the legend for each figure. A P-value <0.05 was accepted as statistically significant.

Results

5-HT-mediated contraction of pulmonary artery rings and [Ca^{2+}] responses in individual smooth muscle cells

Figure 1a shows that 5 μM 5-HT caused a stable contraction in an arterial ring, which recovered fully following 5-HT removal. $5\text{-}HT_{2A}$ receptors were then selectively inhibited with 0.1 μM ketanserin (Yang *et al*., 1994), which did not change the artery tension. However, in the continuous presence of ketanserin,

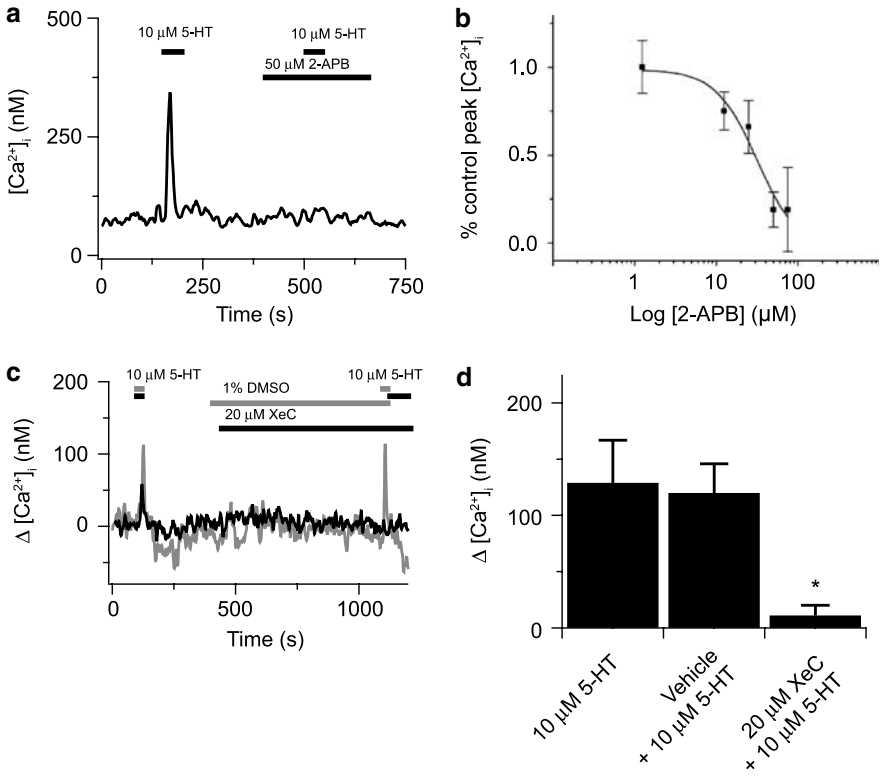

Figure 2 2-APB and XeC block 5-HT-elicited cytosolic $[Ca^{2+}]$ increases in canine PASMCs. (a) 5-HT (10 μM) -induced $[Ca^{2+}]$ transient in the absence and then presence of 50 μM 2-APB. (b) Dose-dependent inhibition of 10 μM 5-HT-induced $[Ca^{2+}]$ transients by 2-APB with an $IC_{50} = 32 \times 10^{-6}$ M (solid line) (equation (1)) based on 22 cells from two animals. (c) 5-HT (10 μM) -induced $[Ca^{2+}]$ transient in the absence and then presence of vehicle carrier (gray line) or 20 μM XeC (solid line). (d) Bars show the magnitude of the peak cytosolic $[Ca^{2+}]$ increase in the absence then presence of 10 μM 5-HT prior to and during vehicle carrier (14 cells) or 20 μM XeC (eight cells from two animals). Values are means of % peak $[Ca^{2+}]$. *Significant difference ($P<0.05$) between XeC and vehicle and 5-HT groups by a Kruskal–Wallis ANOVA on ranks with a Dunn's multiple comparison procedure. Error bars represent $\pm$s.e.m.

5 μM 5-HT did not induce any contraction. Where 5-HT receptor activation caused an average tension increase of 2.54 ± 0.59 g in the absence of ketanserin for five arteries isolated from three animals, 0.1–1 μM ketanserin caused a significant reduction in the tension developed (0.07 ± 0.05 g) ($P<0.05$, paired t-test). Figure 1b shows that 10 μM 5-HT caused cytosolic $[Ca^{2+}]$ to elevate rapidly and transiently in an individual cell. However, in the presence of 0.1 μM ketanserin 10 μM 5-HT failed to elicit any rise in cytosolic $[Ca^{2+}]$. 5-HT (10 μM) caused an average increase in cytosolic $[Ca^{2+}]$ of 116 ± 29 nM for 11 cells isolated from three animals, while in the presence of 0.1 μM ketanserin, 10 μM 5-HT caused a substantially smaller rise in cytosolic $[Ca^{2+}]$ of only 19 ± 9 nM ($P<0.05$, paired t-test).

Since these studies rely on measuring changes in artery contraction and Ca^{2+} signaling processes, dose–response curves for 5-HT were established with concentrations from 10^{-9} to 10^{-4} M. Figure 1c and e shows that 10^{-7} M 5-HT produced threshold tension and $[Ca^{2+}]$ increases, which saturated at $\sim 10^{-5}$ M. The EC_{50}'s for tension and $[Ca^{2+}]$ responses were are also similar.

5-HT, SR Ca^{2+} release and contractility

Our previous work demonstrated that canine pulmonary arterial contraction due to PE was dependent on release of $InsP_3$-sensitive, but not caffeine-ryanodine-sensitive Ca^{2+} stores (Jabr *et al*., 1997); thus we wanted to establish whether 5-HT acts through cell signaling pathways common with those induced by PE. Figure 2 shows the effects of $InsP_3$ receptor inhibition on 5-HT-elicited cytosolic $[Ca^{2+}]$ responses in individual PASMCs. Figure 2a shows that the rapid, transient rise in cytosolic $[Ca^{2+}]$ was markedly attenuated by 50 μM 2-APB with an IC_{50} (Figure 2b) comparable to 2APB inhibition of InsP3 receptors (Wu *et al*., 2000). 2-APB (50 μM) failed to reduce 10 mM caffeine-elicited $[Ca^{2+}]$ increases from the control of 292 ± 56 nM in nine cells from a single animal ($P = 0.46$, paired t-test), illustrating the specificity of 2-APB to block $InsP_3$- and not ryanodine receptor-elicited Ca^{2+} release. The effects of XeC on 5-HT-elicited cytosolic $[Ca^{2+}]$ responses were also determined. Cells were exposed to 20 μM XeC or DMSO or MeOH vehicle for 10–15 min prior to 5-HT exposure. Figure 2c shows that in a single PASMC 10 μM 5-HT induced cytosolic $[Ca^{2+}]$ increases of similar amplitude in the absence and then presence of vehicle carrier (1% DMSO ($v\,v^{-1}$), Gray line). In a separate experiment, 10 μM 5-HT failed to elicit any increase in cytosolic $[Ca^{2+}]$ in the presence, but not absence, of 20 μM XeC (Black line). Figure 2d summarizes data illustrating that XeC significantly reduces 5-HT elicited cytosolic $[Ca^{2+}]$ rises.

Figure 3 shows the arterial tension responses to 5-HT when the $InsP_3$- or ryanodine-sensitive Ca^{2+} stores were depleted. Figure 3a shows that inhibition of sarcoplasmic–endoplasmic reticulum Ca^{2+} ATPase (SERCA) -mediated Ca^{2+} uptake

with 20 μM cyclopiazonic acid (CPA) reduced the contraction to 25 μM 5-HT. Figure 3b shows the tension developed by 5 μM 5-HT in an artery ring that was exposed to ryanodine, which inhibits ryanodine receptors and potentially calcium-induced-calcium-release (CICR) mechanisms (Zucchi & Ronca-Testoni, 1997). In comparison to the effects of CPA, ryanodine did not reduce the 5-HT-mediated contraction. However, Figure 3c shows that ryanodine exposure does reduce the tension developed by 15 mM caffeine. Figure 3d summarizes the data obtained from several arteries. CPA (20 μM) reduced the contractile response to 5-HT in 21 arteries from seven animals. Ryanodine, however, did not (eight arteries from three animals) reduce 5-HT-elicited contractions even though it did significantly reduce caffeine-mediated contractions.

5-HT, extracellular Ca^{2+} entry and contractility

The role of extracellular Ca^{2+} entry during 5-HT induced contractions was then assessed. Figure 4A shows that 25 μM 5-HT induced a sustained contraction when the ring was bathed in 1.8 mM Ca^{2+} (solid line), however with extracellular Ca^{2+} removal, 5-HT caused a transient contraction that rapidly declined and stabilized (dashed line). This slight, sustained, contraction may be due to sensitization of the contractile proteins (Kuriyama *et al*., 1998) since removal of extracellular Ca^{2+} in Ca^{2+}-imaging experiments (see Figure 6a) reduced cytosolic [Ca^{2+}] to basal levels. Figure 4b shows that 10 μM nisoldipine (dashed line) caused the 5-HT-elicited tension to be reduced compared to control (solid line). Figure 4c shows that 100 μM Gd^{3+}, a nonselective cation channel blocker (Hescheler & Schultz, 1993), had no effect on the contraction induced by 25 μM 5-HT.

The summarized data in Figure 4d illustrate that extracellular Ca^{2+} entry is important during 5-HT-induced contractions of pulmonary arterial rings. Each panel shows the mean change in the sustained arterial ring tension due to 5-HT in response to Ca^{2+} entry inhibition. Extracellular Ca^{2+} removal (15 arteries, three animals) caused a dramatic reduction in contractility, while nisoldipine (11 arteries, four animals) reduced the contractility by a smaller amount and Gd^{3+} (six arteries, duplicate animals) had no effect at all. These results implicate roles for both voltage-dependent and voltage-independent Ca^{2+} entry mechanisms during 5-HT-mediated contractions. However, cation channels inhibited by Gd^{3+} are not involved in 5-HT-mediated contractions.

Intracellular [Ca^{2+}] was measured in isolated canine PASMCs in order to better define the roles for different Ca^{2+} entry pathways involved during prolonged 5-HT stimulation. Figure 5a shows that 10 μM 5-HT caused cytosolic [Ca^{2+}] oscillations in an individual myocyte that persisted as long as the agonist was present. Figure 5b, however, shows that in a separate cell 10 μM 5-HT induced an elevation in basal cytosolic [Ca^{2+}] of $\sim$30 nM in addition to cytosolic Ca^{2+} oscillations. There was substantial heterogeneity in the responsiveness of individual cells to 5-HT, though 45 of 48 cells (94%) were responsive. [Ca^{2+}] oscillations alone were

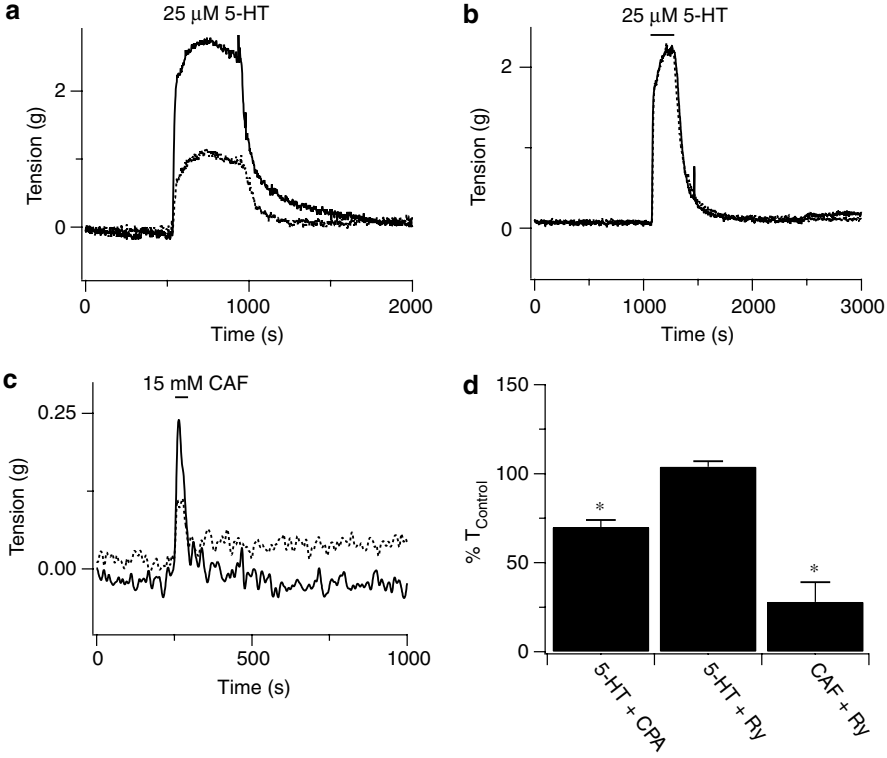

Figure 3 Depletion of intracellular Ca^{2+} stores alters contractile tension responses to 5-HT. (a) 5-HT (5 μM) -induced increase in arterial ring tension in the absence (solid line) or presence (dashed line) of 20 μM CPA. (b) 5-HT (5 μM) -increase in arterial ring tension in the absence (solid line) or presence (dashed line) of 10 μM ryanodine. (c) Caffeine (15 mM) -induced increase in arterial ring tension in the absence (solid line) or presence (dashed line) of 10 μM ryanodine. (d) Mean change in artery tension due to 5-HT or caffeine in the presence of CPA or ryanodine. Error bars represent $\pm$s.e.m. *Means significantly different from their control values by a two-tailed paired *t*-test ($P<0.05$).

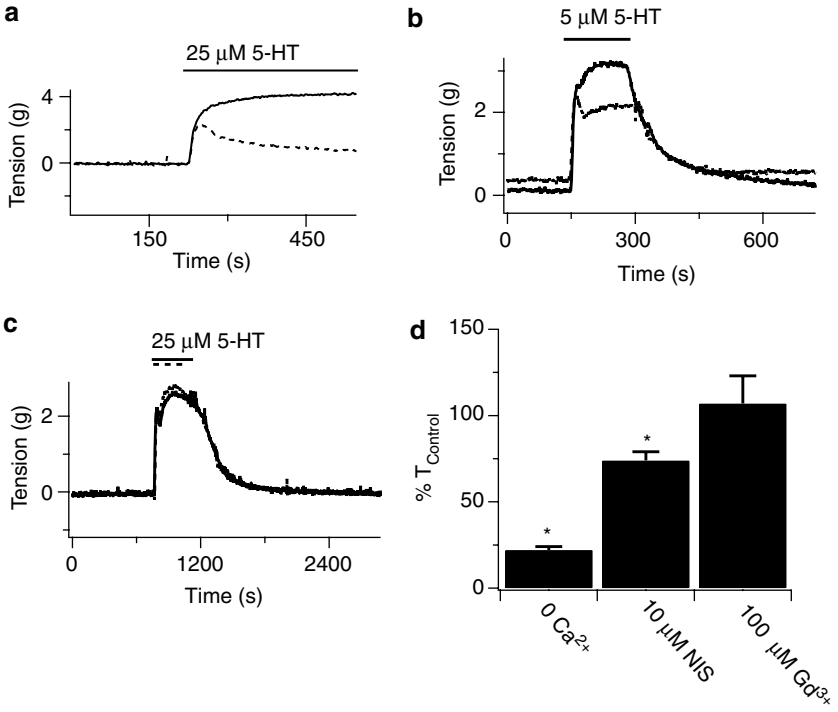

Figure 4 Inhibition of extracellular Ca^{2+} entry reduces 5-HT-induced contractile responses of pulmonary arterial rings. (a) Effect of the presence (solid line) and absence (dashed line) of 1.8 mM extracellular Ca^{2+} on arterial ring tension during 25 μM 5-HT. (b) Effect of the absence (solid line) and presence (dashed line) of 10 μM nisoldipine on arterial ring tension during 5 μM 5-HT. (c) Effect of the absence (solid line) and presence (dashed line) of 100 μM Gd^{3+} on arterial ring tension during 25 μM 5-HT. (d) Mean change in artery tension due to 5-HT in the absence or presence of Ca^{2+} influx pathway inhibition. 5-HT was present at times shown by the bars. Error bars represent $\pm$s.e.m. *Means significantly different from control or nisoldipine conditions by a one-way ANOVA with a SNK multiple comparison procedure ($P<0.05$).

observed in 15 cells (33%), 11 cells (24%) exhibited only $[Ca^{2+}]$ elevations, and 19 cells (43%) had rises in cytosolic $[Ca^{2+}]$ as well as $[Ca^{2+}]$ oscillations. Overall, 5-HT increased the basal cytosolic $[Ca^{2+}]$ by 35 ± 8 nM ($n=48$, five animals), while the mean frequency of $[Ca^{2+}]$ oscillations was 0.011 ± 0.0007 Hz in the 34 cells from those animals that exhibited oscillations.

The dependence of 5-HT-mediated Ca^{2+} signaling on extracellular Ca^{2+} entry was then examined. Figure 5c illustrates that the 5-HT-mediated basal cytosolic $[Ca^{2+}]$ increase was reversibly reduced with extracellular Ca^{2+} removal. To test for 5-HT-mediated extracellular Ca^{2+} entry, cells were exposed to 10 mM Ni^{2+}, a putative inhibitor of several extracellular Ca^{2+} entry pathways, including L-type Ca^{2+} channels (McDonald *et al*., 1994), I_{SOC} (Lewis, 1999), and I_{NSC} (Inoue, 1991) as well as CCE in canine PASMCs (Wilson *et al*., 2002b). Figure 5d shows that prior to Ni^{2+} addition, 5-HT caused rapid oscillations and a slight increase in basal cytosolic $[Ca^{2+}]$, while in the presence of Ni^{2+} the cytosolic $[Ca^{2+}]$ decreased and the oscillatory frequency slowed considerably. Figure 5e illustrates that 10 μM nisoldipine also impaired 5-HT-mediated Ca^{2+} signaling. In this cell, 5-HT caused a large, transient, increase in cytosolic $[Ca^{2+}]$ that decreased and stabilized above baseline. Addition of 10 μM nisoldipine in the continued presence of 5-HT caused cytosolic $[Ca^{2+}]$ to decrease and elicited small amplitude $[Ca^{2+}]$ oscillations.

The summarized data in Figure 5 demonstrate that inhibiting Ca^{2+} entry affects 5-HT-mediated $[Ca^{2+}]$ oscillations and $[Ca^{2+}]$ increases. Figure 5f illustrates that extracellular Ca^{2+} removal ($n=8$) or Ni^{2+} exposure ($n=8$) substantially reduced the frequency of $[Ca^{2+}]$ oscillations. Nisoldipine, however, did not affect the $[Ca^{2+}]$ oscillation frequency ($n=12$). Comparatively, Figure 5g illustrates that extracellular Ca^{2+} removal ($n=6$) or Ni^{2+} ($n=7$) or nisoldipine ($n=15$) exposure reduces the 5-HT-mediated cytosolic $[Ca^{2+}]$ increases.

5-HT fails to activate voltage-independent extracellular Ca^{2+} entry, I_{NSC} or I_{SOC}

To identify the pathway(s) of Ca^{2+} entry involved in 5-HT Ca^{2+} signaling, the rate of Mn^{2+} quench of the fura-2 signal was measured. Mn^{2+} is a commonly used probe for studying voltage-independent Ca^{2+} influx pathways since it is permeable through many Ca^{2+}-selective channels (Missiaen *et al*., 1990) including CCE in canine PASMCs (Wilson *et al*., 2002b). Mn^{2+} is not permeable through voltage-dependent Ca^{2+} channels (Hopf *et al*., 1996a), and is unlikely to be transported out of the cytosol into intracellular compartments or extruded from the cell (Gomes & Madeira, 1986). Figure 6a shows the fluorescence intensity in a single PASMC. Addition of Mn^{2+} elicited a linear decrease in the fura-2 fluorescent signal and the rate of fluorescence quench was unchanged by 10 μM 5-HT. Addition of 1 μM ionomycin caused the quench rate to increase dramatically. Overall, 5-HT failed to alter the rate of fura-2 quench by Mn^{2+} which was 0.038 ± 0.006 FI s^{-1}

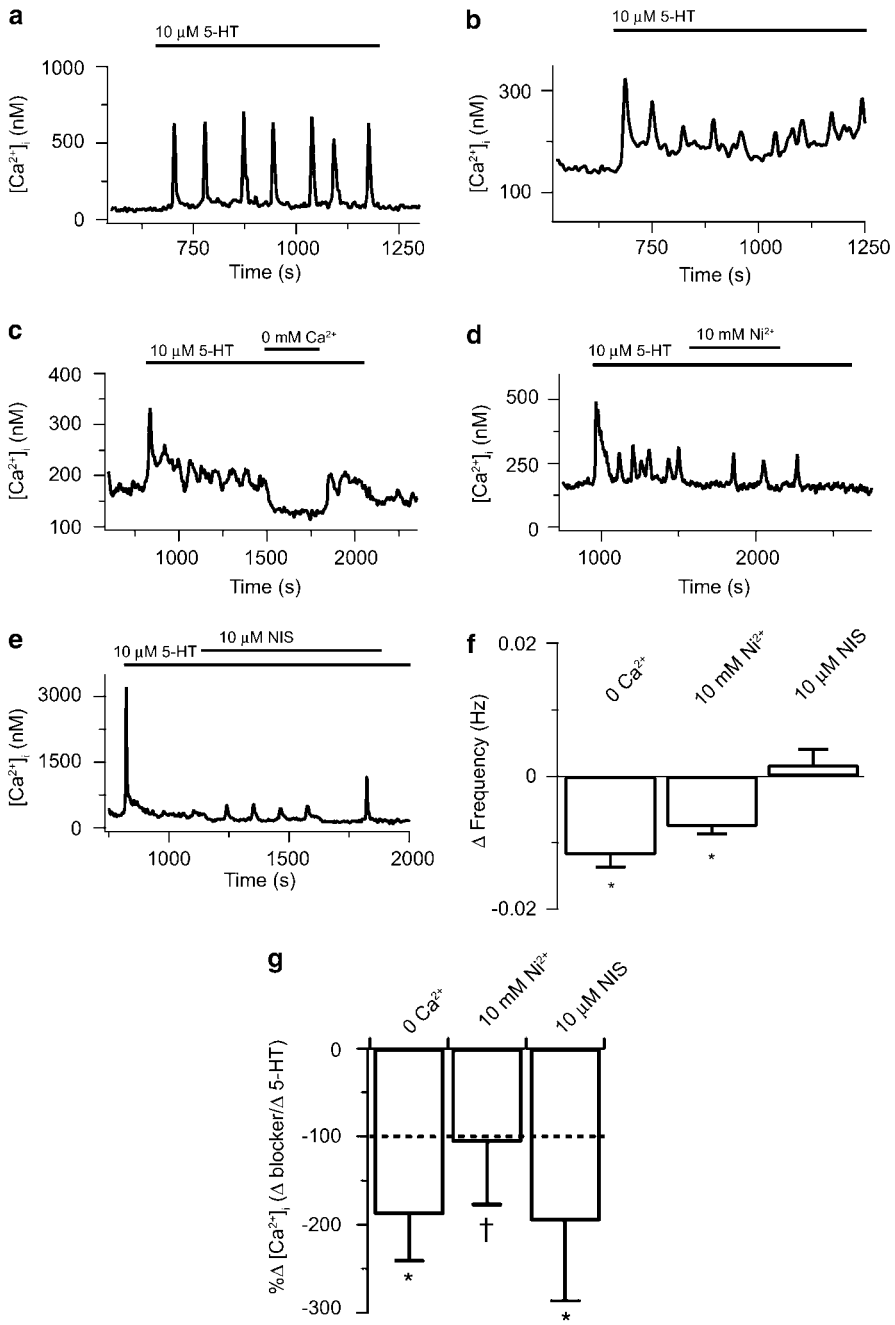

Figure 5 Inhibition of extracellular Ca^{2+} entry influences prolonged 5-HT-mediated Ca^{2+} signaling in single PASMCs. (a) 5-HT (10 μM) -induced cytosolic [Ca^{2+}] oscillations. (b) 5-HT (10 μM) -induced elevation in basal cytosolic [Ca^{2+}] and [Ca^{2+}] oscillations. (c) Effect of Ca^{2+} removal on cytosolic [Ca^{2+}] during 10 μM 5-HT. (d) Effect of 10 mM Ni^{2+} on cytosolic [Ca^{2+}] during 10 μM 5-HT. (e) Effect of 10 μM nisoldipine on cytosolic [Ca^{2+}] during 10 μM 5-HT. (f) Mean change in [Ca^{2+}] oscillatory frequency due to 5-HT in the absence or presence of Ca^{2+} influx pathway inhibition. (g) Change in cytosolic [Ca^{2+}] during Ca^{2+} influx pathway inhibition in the presence of 5-HT measured relative to the change in cytosolic [Ca^{2+}] measured during 5-HT alone. Dashed line represents the basal cytosolic [Ca^{2+}]. Error bars represent $\pm$s.e.m. Agonists were present at times shown by the bars. Means significantly different from their controls by *a two-tailed paired *t*-test or †signed rank test ($P<0.05$).

prior to and 0.032 ± 0.005 FI s^{-1} in the presence of 5-HT (19 cells, three animals, $P=0.20$, paired *t*-test).

Voltage-clamp experiments were also performed to determine if 5-HT directly activates I_{NSC} or indirectly activates I_{SOC} since Mn^{2+} may not be permeable through all types of noncapacitative calcium entry pathways (NCCE) (Broad *et al.*, 1999). Membrane currents were recorded from single canine PASMCs using the dialyzed whole-cell patch-clamp configuration. Cells were held at a potential of 0 mV and stepped to -60 mV for 200 ms every 15 s to monitor current activation in the presence of 2 mM external Ca^{2+}. Figure 6b shows representative membrane currents before and during exposure of the cell to 10 μM 5-HT. In this cell, and in four additional cells, 5-HT exposure failed to activate I_{NSC}.

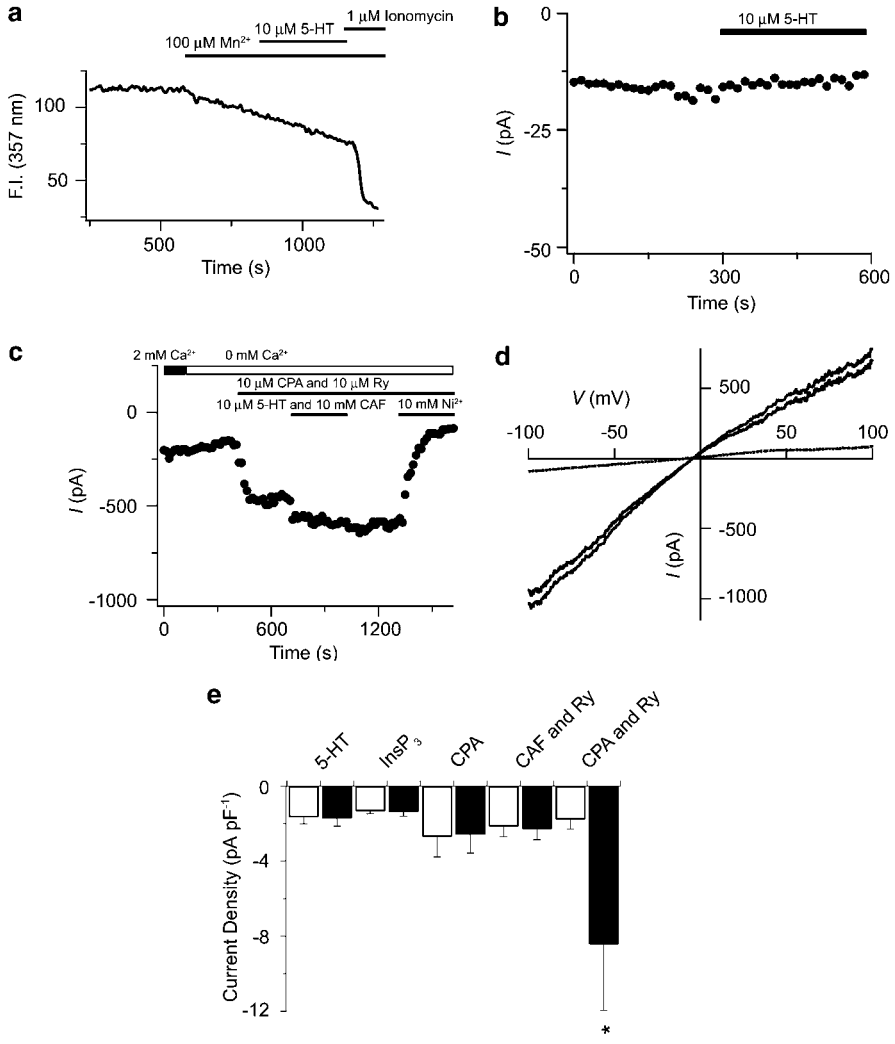

Figure 6 Depletion of SR Ca^{2+} stores but not 5-HT activates I_{NSC}. (a) 5-HT (10 μM) and ionomycin (1 μM) effects on fura-2 quench by Mn^{2+}. (b) Lack of effect of 10 μM 5-HT on membrane currents in PASMC. (c) Intracellular Ca^{2+} store-depletion-induced nonselective cation currents in the absence and presence of 10 mM Ni^{2+}. (d) Representative currents in response to a 180 ms voltage ramp from -100 to $+100$ mV from a single PASMC before (dashed line) and after (gray line) store depletion. I_{SOC} current amplitude (black line) obtained by subtracting currents before store depletion from currents following store depletion. Cells were held at 0 mV and stepped every 15 s to -60 mV for 200 ms in (b, c). (e) Simultaneous depletion of $InsP_3$ and caffeine–ryanodine-sensitive intracellular Ca^{2+} stores is required to activate I_{SOC}. Bars show the mean current density measured at a potential of -60 mV before (open bars) and after releasing or depleting the intracellular Ca^{2+} stores (black). See text for experimental details. Error bars represent $\pm$s.e.m. Agonists were present at times shown by the bars. *Means significantly different from their controls by a two-tailed paired *t*-test test ($P<0.05$).

Simultaneous depletion of $InsP_3$- and ryanodine-sensitive intracellular Ca^{2+} stores activates I_{SOC} in canine PASMCs

The inability of 5-HT to increase the Mn^{2+} quench rate as well as the lack of I_{NSC} activation suggests that 5-HT does not enhance voltage-independent Ca^{2+} entry. We therefore confirmed the presence of nonselective cation currents by eliciting those activated in response to store depletion. We have recently shown that simultaneous depletion of the functionally independent $InsP_3$ and caffeine ryanodine-sensitive intracellular Ca^{2+} stores causes an increase in both the cytosolic [Ca^{2+}] and Mn^{2+} quench rate (Wilson *et al*., 2002b) and Ng and Gurney (2001) demonstrated that depletion of the SR Ca^{2+} stores of rat PASMCs elicits I_{SOC}. Figure 6c shows results from experiments that demonstrate that SR Ca^{2+} store depletion is indeed capable of activating I_{SOC} in canine PASMCs. After the whole-cell current stabilized (2–5 min after gaining access) the intracellular Ca^{2+} stores were maximally depleted by exposing cells to a cocktail including 10 μM CPA, 10 μM ryanodine and briefly exposing cells to 10 μM 5-HT and 10 mM CAF. This procedure is similar to the ones we have used previously in canine pulmonary arteries and PASMCs to deplete both $InsP_3$ and caffeine–ryanodine-sensitive intracellular Ca^{2+} stores (Jabr *et al*., 1997; Janiak *et al*., 2001) and to activate CCE (Wilson *et al*., 2002b). To rule out any direct activation or inhibition of membrane currents by 5-HT and caffeine, these agonists were washed out for 5 minutes and the currents were recorded in the continued presence of CPA plus ryanodine. The panel illustrates that simultaneous depletion of both the $InsP_3$ and caffeine-sensitive intracellular Ca^{2+} stores activated an inward current at a potential of -60 mV. Figure 6c also

shows that 10 mM Ni^{2+} significantly inhibited the amplitude of I_{SOC} activated by simultaneous Ca^{2+} store depletion, which is analogous to Ni^{2+} inhibition of CCE in canine PASMCs (Wilson *et al*., 2002b). On average, depletion of the $InsP_3$-and ryanodine-sensitive Ca^{2+} stores caused a significant increase from -3.5 ± 2.7 pA pF^{-1} to -28.6 ± 11.2 pA pF^{-1} in current density, and 10 mM Ni^{2+} significantly reduced this store-depletion-induced current to -7.7 ± 5.2 pA pF^{-1}, which is not significantly different from basal values ($n=6$). Figure 6d shows the currents recorded in response to a 180 ms voltage ramp protocol from -100 to $+100$ mV under control conditions and after depletion of both intracellular Ca^{2+} stores in individual canine PASMCs performed in the absence of extracellular Ca^{2+}. Depletion of the $InsP_3$ and caffeine–ryanodine-sensitive Ca^{2+} stores activated a membrane current with a small amount of inward rectification and a reversal potential near 0 mV.

Figure 6e summarizes the data showing the effect of releasing or depleting the $InsP_3$ or caffeine–ryanodine-sensitive intracellular Ca^{2+} stores separately or together since CCE in canine PASMCs is activated only with simultaneous depletion of both intracellular Ca^{2+} stores (Wilson *et al*., 2002b). Release of the $InsP_3$-sensitive intracellular Ca^{2+} store, either by 5-HT receptor activation as illustrated in Figure 6b or by direct $InsP_3$ receptor stimulation with intracellular perfusion of 10 μM $InsP_3$, is insufficient to activate I_{SOC} at a potential of -60 mV ($n=9$). Selective depletion of the $InsP_3$-sensitive store by perfusion of 10 μM CPA also failed to activate I_{SOC} at a potential of -60 mV ($n=7$). Similarly, selective depletion of the caffeine–ryanodine-sensitive intracellular Ca^{2+} store alone by perfusing the cells with 10 mM caffeine and 10 μM ryanodine (Janiak *et al*., 2001) also did not activate I_{SOC} ($n=9$). Only simultaneous depletion of both the $InsP_3$- and caffeine–ryanodine-sensitive intracellular Ca^{2+} stores resulted in significant I_{SOC} activation.

Role of constitutively active, Ni^{2+}-sensitive, Ca^{2+} entry pathway in canine PASMCs

The final series of experiments were designed to determine whether canine PASMCs have constitutively active, Ni^{2+}-sensitive Ca^{2+} entry pathways (Albert *et al*., 2003), since the 5-HT-mediated cytosolic [Ca^{2+}] increases and [Ca^{2+}] oscillations are sensitive to Ni^{2+} (Figure 5), but do not appear to involve activation of I_{NSC} or I_{SOC} (Figure 6). Figure 7 shows the basal Mn^{2+} quench rate of fura-2 in unstimulated cells, and its sensitivity to a number of inhibitors. Figure 7a illustrates that 10 mM Ni^{2+} nearly abolishes Mn^{2+} quench of the fura-2 signal. Moreover, with Ni^{2+} removal the quench rate increased to the control quench rate, indicating that the block of Mn^{2+} quench by Ni^{2+} is readily reversible. Figure 7b and c show representative experiments illustrating that 10 μM nisoldipine or 100 μM Gd^{2+} do not alter the basal quench rate. Figure 7d summarizes the data indicating that Ni^{2+} markedly reduced the rate of Mn^{2+} entry ($n=21$), while 10 μM nisoldipine ($n=3$) or Gd^{3+} ($n=7$) failed to significantly alter the rate of Mn^{2+} quench.

Discussion

There are several major findings to this work. 5-HT-elicited cytosolic [Ca^{2+}] increases were inhibited by XeC as well as 2-APB; thus, activation of $InsP_3$ receptors is critical to the

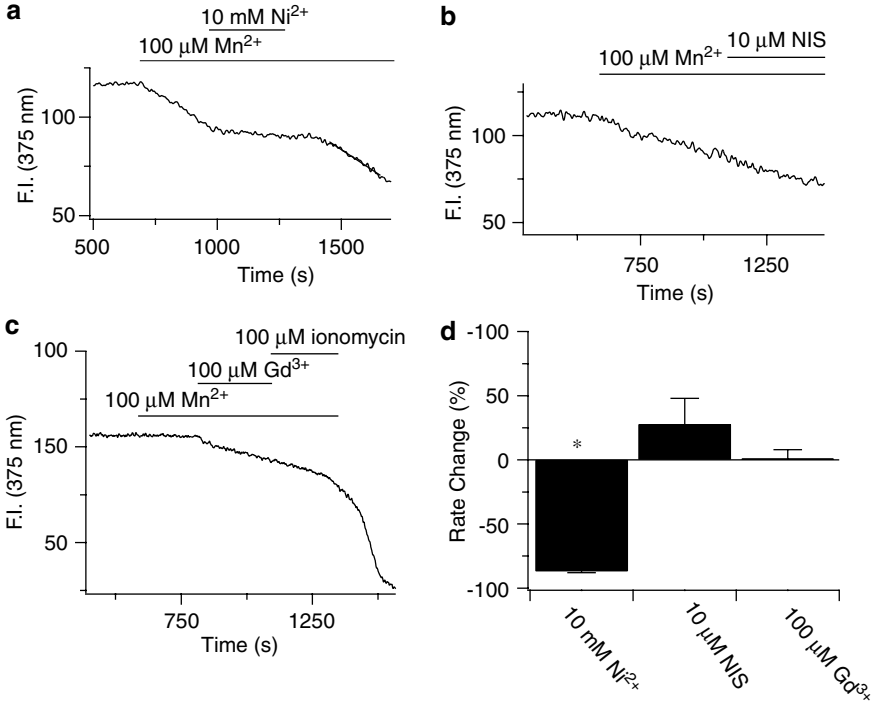

Figure 7 Ni^{2+} but not nisoldipine or Gd^{3+} reduces the rate of Mn^{2+} entry in canine PASMCs. (a) Effect of 10 mM Ni^{2+} on fura-2 quench by Mn^{2+}. (b) Effect of 10 μM nisoldipine on fura-2 quench by Mn^{2+}. (c) Effect of 100 μM Gd^{3+} on fura-2 quench by Mn^{2+}. (d) Percent change in fura-2 quench rate by Mn^{2+} compared to control. Agonists were present at times shown by the bars. Error bars represent $\pm$s.e.m. *Means significantly different from their controls by a two-tailed paired *t*-test ($P<0.05$).

initiation of cytosolic [Ca^{2+}] rises. During 5-HT stimulation of canine pulmonary arteries, constitutively active Ca^{2+} permeation pathways along with L-type Ca^{2+} channels contribute to Ca^{2+} signaling and contractility. Although there was no evidence for 5-HT activation of I_{NSC} or I_{SOC}, simultaneous depletion of both SR Ca^{2+} stores activated I_{SOC}, which is likely to be responsible for the recently described CCE in these cells (Wilson *et al*., 2002b).

Receptor-mediated cytosolic [Ca^{2+}] increases and oscillations are often due to release of $InsP_3$-sensitive Ca^{2+} stores (Thomas *et al*., 1995; 1996) and this holds for 5-HT-elicited contractility and cytosolic [Ca^{2+}] increases in canine pulmonary arteries and smooth muscle cells. Selective depletion of the caffeine–ryanodine-sensitive Ca^{2+} store failed to affect the contraction induced by 5-HT, and 5-HT-elicited [Ca^{2+}] rises were blocked by the $InsP_3$ receptor inhibitors 2-APB and XeC. These findings parallel our previously published studies where PE-induced contractions (Jabr *et al*., 1997) and angiotensin-mediated cytosolic [Ca^{2+}] increases (Janiak *et al*., 2001) were also unaffected by selective depletion of the caffeine–ryanodine-sensitive Ca^{2+} stores.

5-HT can induce membrane potential oscillations that activate L-type Ca^{2+} channels, facilitating [Ca^{2+}] oscillations as well as contractility (Kuriyama *et al*., 1998). In canine pulmonary arteries, 5-HT-mediated contractions are dependent on both nisoldipine-sensitive as well as nisoldipine-insensitive Ca^{2+} entry. The lack of an increase in Mn^{2+} quench with 5-HT exposure does not contradict any potential involvement of L-type Ca^{2+} channels in the 5-HT response as Mn^{2+} does not readily permeate L-type Ca^{2+} channels (Hopf *et al*., 1996a). The lack of an effect of nisoldipine on 5-HT-mediated [Ca^{2+}] oscillations signifies that L-type Ca^{2+} channels play little, if any, role in the maintenance of these [Ca^{2+}] oscillations. Assuming the oscillatory behavior is due to $InsP_3R$ activation, these data also suggest that Ca^{2+} flux through L-type channels is not involved in $InsP_3$ Ca^{2+} stores refilling in canine pulmonary ASMCs.

The finding that 5-HT stimulation did not activate I_{SOC} or I_{NSC} in canine PASMCs contrasts with the work of other groups and was unexpected. PE stimulation of swine renal arteries activates CCE that is important in the maintenance of tone (Utz *et al*., 1999). Similarly, norepinephrine activates I_{NSC} in rabbit portal vein (Helliwell & Large, 1997). Mn^{2+}-permeable CCE and non-Mn^{2+}-permeable NCCE Ca^{2+} entry pathways are activated in A7R5 smooth muscle cells by arginine vasopressin (Broad *et al*., 1999). Recently, our group reported that mRNA for canonical transient receptor potential (TRPC) channels, a class of nonselective cation channels that may be the molecular correlates of NCCE and CCE are expressed in canine PASMCs (Walker *et al*., 2001). Specifically, TRPC4, TRPC6, and TRPC7 are expressed while TRPC1, TRPC2, TRPC3, and TRPC5 are not. Our expectation was that 5-HT would activate I_{NSC} because G-protein-coupled receptors and DAGs activate portal vein I_{NSC} (Helliwell & Large, 1997) as well as TRPC6 and TRPC7 independent of Ca^{2+} store depletion (Hofmann *et al*., 1999; Okada *et al*., 1999; McKay *et al*., 2000). TRPC4 in comparison can be activated by depletion of the intracellular Ca^{2+} stores (Walker *et al*., 2002), and may therefore be involved in I_{SOC} and CCE responses in canine PASMCs.

The current study provides evidence that depletion of SR Ca^{2+} stores activates I_{SOC} in canine PASMC. The finding that depletion of intracellular Ca^{2+} stores activates I_{SOC} complements work by other researchers in PASMC (Ng & Gurney, 2001) and many other vascular smooth muscle cells, including rabbit portal vein (Albert & Large, 2002), mouse aorta (Trepakova *et al*., 2001), and mouse anococcygeus (Wayman *et al*., 1999). However, the uniqueness of this response in canine PASMCs relates to the requirement that only simultaneous depletion of both the $InsP_3$- and ryanodine-sensitive intracellular Ca^{2+} stores activates CCE (Jabr *et al*., 1997; Janiak *et al*., 2001; Wilson *et al*., 2002b). Thus, the unique organization of functionally distinct ryanodine- and $InsP_3$-sensitive intracellular Ca^{2+} stores in canine PASMC explains why 5-HT-induced Ca^{2+} release from $InsP_3$-sensitive Ca^{2+} stores fails to activate CCE. In other smooth muscle cell types, where $InsP_3$ receptors and ryanodine receptors share a common intracellular Ca^{2+} store, 5-HT would likely activate CCE. An example is canine renal arterial smooth cells, where ryanodine- and $InsP_3$-sensitive Ca^{2+} stores exhibit significant overlap (Wilson *et al*., 2002b). It is likely, however, that the unusual organization of intracellular Ca^{2+} stores and the inability of 5-HT alone to activate CCE in canine PASMCs may not be a unique property associated only with the pulmonary circulation, since it appears that ryanodine and $InsP_3$ receptors share a common Ca^{2+} store in rat PASMCs, where 5-HT has been shown to activate CCE (Yuan *et al*., 1997; Ng & Gurney, 2001). In contrast, in cultured fetal rat aortic cells (A7r5), which also exhibit functionally distinct ryanodine- and $InsP_3$-sensitive intracellular Ca^{2+} stores (Tribe *et al*., 1994), 5-HT actions may resemble those in canine PASMC.

The results illustrate that, during 5-HT stimulation of canine pulmonary arteries and cells, Ca^{2+} signaling and contractility are reliant on both voltage-dependent as well as voltage-independent Ca^{2+} entry. However, the lack of CCE or NCCE activation by 5-HT strongly suggests that constitutively active Ca^{2+} entry pathways are important to intracellular Ca^{2+} store refilling and vasoconstriction. Since Ni^{2+} inhibits basal Ca^{2+} entry in canine PASMCs (Wilson *et al*., 2002b) as well as 5-HT-mediated [Ca^{2+}] responses and unstimulated Mn^{2+} quench in the present studies, basal Ca^{2+} entry may replenish the SR Ca^{2+} stores during 5-HT exposure. There is precedent for the involvement of Ca^{2+} leak currents during muscle contraction (Williams, 1990; Alderton & Steinhardt, 2000) and Ca^{2+} leak currents may be store-operated channels that are constitutively active (Fong *et al*., 1990; Hopf *et al*., 1996a, b).

Whole-cell and single-channel recordings of constitutively active nonselective cation channels have been performed in a number of smooth muscle preparations. Rabbit PASMCs have a constitutively active nonselective cation channel that contributes to the resting membrane potential and Na^+ entry (Bae *et al*., 1999). Guinea-pig ear artery SMCs in comparison have nonselective cation channels that are active under basal conditions and are Ca^{2+} permeable (Albert *et al*., 2003). In canine PASMCs, constitutively active Ca^{2+} entry pathways may therefore underlie the previously described basal Ca^{2+} entry pathways blocked by Ni^{2+} (Wilson *et al*., 2002b) that we now show to be Mn^{2+} permeable. The data presented here provide evidence that these basal Ca^{2+} entry pathways have important roles in SR Ca^{2+} store refilling and the maintenance of Ca^{2+} signaling and contractility in response to $5HT_{2A}$ receptor stimulation.

We thank Dr Linda Ye, Phillip Keller, and Shen Xiao-Ming for technical assistance. We also thank Dr Greg Smith for insightful discussions. This work was supported by National Heart Lung and Blood Institute Grants HL-48254 (JRH) and HL-10476 (SMW), and P20 RR15581 from the National Center for Research Resources.

References

AHN, D.S. & HUME, J.R. (1997). pH regulation of voltage-dependent K^+ channels in canine pulmonary arterial smooth muscle cells. *Pflugers Archiv. Eur. J. Physiol.,* **433,** 758–765.

ALBERT, A.P. & LARGE, W.A. (2002). A Ca^{2+}-permeable non-selective cation channel activated by depletion of internal Ca^{2+} stores in single rabbit portal vein myocytes. *J. Physiol.,* **538,** 717–728.

ALBERT, A.P., PIPER, A.S. & LARGE, W.A. (2003). Properties of a constitutively active Ca^{2+}-permeable non-selective cation channel in rabbit ear artery myocytes. *J. Physiol.,* **549,** 143–156.

ALDERTON, J.M. & STEINHARDT, R.A. (2000). How calcium influx through calcium leak channels is responsible for the elevated levels of calcium-dependent proteolysis in dystrophic myotubes. *Trends Cardiovasc. Med.,* **10,** 268–272.

BAE, Y.M., PARK, M.K., LEE, S.H., HO, W.K. & EARM, Y.E. (1999). Contribution of Ca^{2+}-activated K^+ channels and non-selective cation channels to membrane potential of pulmonary arterial smooth muscle cells of the rabbit. *J. Physiol.,* **514,** 747–758.

BAYLOR, S.M. & HOLLINGWORTH, S. (2000). Measurement and interpretation of cytoplasmic [Ca^{2+}] signals from calcium-indicator dyes. *News Pharmacol. Sci.,* **15,** 19–26.

BROAD, L.M., CANNON, T.R. & TAYLOR, C.W. (1999). A non-capacitative pathway activated by arachidonic acid is the major Ca^{2+} entry mechanism in rat A7r5 smooth muscle cells stimulated with low concentrations of vasopressin. *J. Physiol.,* **517,** 121–134.

FONG, P.Y., TURNER, P.R., DENETCLAW, W.F. & STEINHARDT, R.A. (1990). Increased activity of calcium leak channels in myotubes of Duchenne human and mdx mouse origin. *Science,* **250,** 673–676.

FURCHGOTT, R.F. & ZAWADZKI, J.V. (1980). The obligatory role of endothelial cells in the relaxation of arterial smooth muscle by acetylcholine. *Nature,* **288,** 373–376.

GAFNI, J., MUNSCH, J.A., LAM, T.H., CATLIN, M.C., COSTA, L.G., MOLINSKI, T.F. & PESSAH, I.N. (1997). Xestospongins: potent membrane permeable blockers of the inositol 1,4,5-trisphosphate receptor. *Neuron,* **19,** 723–733.

GOMES, D.C. & MADEIRA, V.M. (1986). Magnesium and manganese ions modulate Ca^{2+} uptake and its energetic coupling in sarcoplasmic reticulum. *Archiv. Biochem. Biophys.,* **249,** 199–206.

GRYNKIEWICZ, G., POENIE, M. & TSIEN, R.Y. (1985). A new generation of Ca^{2+} indicators with greatly improved fluorescence properties. *J. Biol. Chem.,* **260,** 3440–3450.

HAMILL, O.P., MARTY, A., NEHER, E., SAKMANN, B. & SIGWORTH, F.J. (1981). Improved patch-clamp techniques for high-resolution current recording from cells and cell-free membrane patches. *Pflugers Archiv. Eur. J. Physiol.,* **391,** 85–100.

HELLIWELL, R.M. & LARGE, W.A. (1997). Alpha 1-adrenoceptor activation of a non-selective cation current in rabbit portal vein by 1,2-diacyl-sn-glycerol. *J. Physiol.,* **499,** 417–428.

HESCHELER, J. & SCHULTZ, G. (1993). Nonselective cation channels: physiological and pharmacological modulations of channel activity. *EXS,* **66,** 27–43.

HOFMANN, T., OBUKHOV, A.G., SCHAEFER, M., HARTENECK, C., GUDERMANN, T. & SCHULTZ, G. (1999). Direct activation of human TRPC6 and TRPC3 channels by diacylglycerol. *Nature,* **397,** 259–263.

HOPF, F.W., REDDY, P., HONG, J. & STEINHARDT, R.A. (1996a). A capacitative calcium current in cultured skeletal muscle cells is mediated by the calcium-specific leak channel and inhibited by dihydropyridine compounds. *J. Biol. Chem.,* **271,** 22358–22367.

HOPF, F.W., TURNER, P.R., DENETCLAW JR, W.F., REDDY, P. & STEINHARDT, R.A. (1996b). A critical evaluation of resting intracellular free calcium regulation in dystrophic mdx muscle. *Am. J. Physiol. Cell Physiol.,* **271,** C1325–C1339.

INOUE, R. (1991). Effect of external Cd^{2+} and other divalent cations on carbachol-activated non-selective cation channels in guinea-pig ileum. *J. Physiol.,* **442,** 447–463.

JABR, R.I., TOLAND, H., GELBAND, C.H., WANG, X.X. & HUME, J.R. (1997). Prominent role of intracellular Ca^{2+} release in hypoxic vasoconstriction of canine pulmonary artery. *Br. J. Pharmacol.,* **122,** 21–30.

JANIAK, R., WILSON, S.M., MONTAGUE, S. & HUME, J.R. (2001). Heterogeneity of calcium stores and elementary release events in canine pulmonary arterial smooth muscle cells. *Am. J. Physiol. Cell Physiol.,* **280,** C22–C33.

KISELYOV, K., XU, X., MOZHAYEVA, G., KUO, T., PESSAH, I., MIGNERY, G., ZHU, X., BIRNBAUMER, L. & MUALLEM, S. (1998). Functional interaction between $InsP_3$ receptors and store-operated Htrp3 channels. *Nature,* **396,** 478–482.

KURIYAMA, H., KITAMURA, K., ITOH, T. & INOUE, R. (1998). Physiological features of visceral smooth muscle cells, with special reference to receptors and ion channels. *Physiol. Rev.,* **78,** 811–920.

LARGE, W.A. (1991). Three membrane-conductance mechanisms activated by noradrenaline in vascular smooth muscle. *Z. Kardiol.,* **80** (Suppl 7), 55–57.

LEWIS, R.S. (1999). Store-operated calcium channels. *Adv. Second Messenger Phosphoprot. Res.,* **33,** 279–307.

MA, H.T., PATTERSON, R.L., VAN ROSSUM, D.B., BIRNBAUMER, L., MIKOSHIBA, K. & GILL, D.L. (2000). Requirement of the inositol trisphosphate receptor for activation of store-operated Ca(2+) channels. *Science,* **287,** 1647–1651.

MACLEAN, M.R., HERVE, P., EDDAHIBI, S. & ADNOT, S. (2000). 5-hydroxytryptamine and the pulmonary circulation: receptors, transporters and relevance to pulmonary arterial hypertension. *Br. J. Pharmacol.,* **131,** 161–168.

MCDANIEL, S.S., PLATOSHYN, O., WANG, J., YU, Y., SWEENEY, M., KRICK, S., RUBIN, L.J. & YUAN, J.X.J. (2001). Capacitative Ca^{2+} entry in agonist-induced pulmonary vasoconstriction. *Am. J. Physiol. Lung Cell Mol. Physiol.,* **280,** L870–L880.

MCDONALD, T.F., PELZER, S., TRAUTWEIN, W. & PELZER, D.J. (1994). Regulation and modulation of calcium channels in cardiac, skeletal, and smooth muscle cells. *Physiol. Rev.,* **74,** 365–507.

MCGOON, M.D. & VANHOUTTE, P.M. (1984). Aggregating platelets contract isolated canine pulmonary arteries by releasing 5-hydroxytryptamine. *J. Clin. Invest.,* **74,** 828–833.

MCKAY, R.R., SZYMECZEK-SEAY, C.L., LIEVREMONT, J.P., BIRD, G.S., ZITT, C., JUNGLING, E., LUCKHOFF, A. & PUTNEY, J.W. (2000). Cloning and expression of the human transient receptor potential 4 (TRP4) gene: localization and functional expression of human TRP4 and TRP3. *Biochem. J.,* **351,** 735–746.

MISSIAEN, L., DECLERCK, I., DROOGMANS, G., PLESSERS, L., DE SMEDT, H., RAEYMAEKERS, L. & CASTEELS, R. (1990). Agonist-dependent Ca^{2+} and Mn^{2+} entry dependent on state of filling of Ca^{2+} stores in aortic smooth muscle cells of the rat. *J. Physiol.,* **427,** 171–186.

NG, L.C. & GURNEY, A.M. (2001). Store-operated channels mediate Ca(2+) influx and contraction in rat pulmonary artery. *Circ. Res.,* **89,** 923–929.

OKADA, T., INOUE, R., YAMAZAKI, K., MAEDA, A., KUROSAKI, T., YAMAKUNI, T., TANAKA, I., SHIMIZU, S., IKENAKA, K., IMOTO, K. & MORI, Y. (1999). Molecular and functional characterization of a novel mouse transient receptor potential protein homologue TRP7. Ca(2+)-permeable cation channel that is constitutively activated and enhanced by stimulation of G protein-coupled receptor. *J. Biol. Chem.,* **274,** 27359–27370.

RAE, J., COOPER, K., GATES, P. & WATSKY, M. (1991). Low access resistance perforated patch recordings using amphotericin B. *J. Neurosci. Methods,* **37,** 15–26.

THOMAS, A.P., BIRD, G.S., HAJNOCZKY, G., ROBB-GASPERS, L.D. & PUTNEY, J.W. (1996). Spatial and temporal aspects of cellular calcium signaling. *FASEB J.,* **10,** 1505–1517.

THOMAS, A.P., ROBB-GASPERS, L.D., ROONEY, T.A., HAJNOCZKY, G., RENARD-ROONEY, D.C. & LIN, C. (1995). Spatial organization of oscillating calcium signals in liver. *Biochem. Soc. Trans.,* **23,** 642–648.

TREPAKOVA, E.S., GERICKE, M., HIRAKAWA, Y., WEISBROD, R.M., COHEN, R.A. & BOLOTINA, V.M. (2001). Properties of a native cation channel activated by Ca^{2+} store depletion in vascular smooth muscle cells. *J. Biol. Chem.,* **276,** 7782–7790.

TRIBE, R.M., BORIN, M.L. & BLAUSTEIN, M.P. (1994). Functionally and spatially distinct Ca^{2+} stores are revealed in cultured vascular smooth muscle cells. *Proc. Natl. Acad. Sci. U.S.A.,* **91,** 5908–5912.

UTZ, J., ECKERT, R. & TRAUTWEIN, W. (1999). Changes of intracellular calcium concentrations by phenylephrine in renal arterial smooth muscle cells. *Pflugers Archiv. Eur. J. Physiol.,* **438,** 725–731.

WALKER, R.L., KOH, S.D., SERGEANT, G.P., SANDERS, K.M. & HOROWITZ, B. (2002). TRPC4 currents have properties similar to the pacemaker current in interstitial cells of Cajal. *Am. J. Physiol. Cell Physiol.,* **283,** C1637–C1645.

WALKER, R.L., HUME, J.R. & HOROWITZ, B. (2001). Differential expression and alternative splicing of TRP channel genes in smooth muscles. *Am. J. Physiol. Cell Physiol.,* **280,** C1184–C1192.

WAURICK, R., KNAPP, J., VAN AKEN, H., BOKNIK, P., NEUMANN, J. & SCHMITZ, W. (1999). Effect of 2,3-butanedione monoxime on force of contraction and protein phosphorylation in bovine smooth muscle. *Naunyn-Schmiedeberg's Archiv. Pharmacol.,* **359,** 484–492.

WAYMAN, C.P., WALLACE, P., GIBSON, A. & MCFADZEAN, I. (1999). Correlation between store-operated cation current and capacitative Ca^{2+} influx in smooth muscle cells from mouse anococcygeus. *Eur. J. Pharmacol.,* **376,** 325–329.

WELSH, D.G., NELSON, M.T., ECKMAN, D.M. & BRAYDEN, J.E. (2000). Swelling-activated cation channels mediate depolarization of rat cerebrovascular smooth muscle by hyposmolarity and intravascular pressure. *J. Physiol.,* **527,** 139–148.

WILLIAMS, J.H. (1990). Depression of posttetanic twitch potentiation by low calcium and calcium channel antagonists. *J. Appl. Physiol.,* **69,** 1093–1097.

WILSON, S.M., JOHNSTON, L., NICHOLSON, N. & HUME, J.R. (2002a). The role of basal Ca^{2+} entry during serotonin mediated Ca^{2+} entry in pulmonary arterial smooth muscle cells. *FASEB J.,* **16**, 870.1.

WILSON, S.M., MASON, H.S., SMITH, G.D., NICHOLSON, N., JOHNSTON, L., JANIAK, R. & HUME, J.R. (2002b). Comparative capacitative calcium entry mechanisms in canine pulmonary and renal arterial smooth muscle cells. *J. Physiol.,* **543,** 917–931.

WU, J., KAMIMURA, N., TAKEO, T., SUGA, S., WAKUI, M., MARUYAMA, T. & MIKOSHIBA, K. (2000). 2-Aminoethoxydiphenyl borate modulates kinetics of intracellular Ca(2+) signals mediated by inositol 1,4,5-trisphosphate-sensitive Ca(2+) stores in single pancreatic acinar cells of mouse. *Mol. Pharmacol.,* **58,** 1368–1374.

YANG, C.M., FEN, L.W., TSAO, H.L. & CHIU, C.T. (1997). Inhibition of 5-hydroxytryptamine-induced phosphoinositide hydrolysis and Ca^{2+} mobilization in canine cultured tracheal smooth muscle cells by phorbol ester. *Br. J. Pharmacol.,* **121,** 853–860.

YANG, C.M., HSIEH, J.T., YO, Y.L., ONG, R. & TSAO, H.L. (1994). 5-Hydroxytryptamine-stimulated calcium mobilization in cultured canine tracheal smooth muscle cells. *Cell Calcium,* **16,** 194–204.

YUAN, X.J., BRIGHT, R.T., ALDINGER, A.M. & RUBIN, L.J. (1997). Nitric oxide inhibits serotonin-induced calcium release in pulmonary artery smooth muscle cells. *Am. J. Physiol. Lung Cell. Mol. Physiol.,* **272,** L44–L50.

ZUCCHI, R. & RONCA-TESTONI, S. (1997). The sarcoplasmic reticulum Ca^{2+} channel/ryanodine receptor: modulation by endogenous effectors, drugs and disease states. *Pharmacol. Rev.,* **49,** 1–51.

ZWEIFACH, A. & LEWIS, R.S. (1995). Slow calcium-dependent inactivation of depletion-activated calcium current. Store-dependent and -independent mechanisms. *J. Biol. Chem.,* **270,** 14445–14451.

(Received August 10, 2004
Revised October 20, 2004
Accepted October 28, 2004)